

# Experimental study and numerical modeling of liquid sloshing damping in a cylindrical container with annular and sectorial baffles

Mohammad Mahdi Mohammadi<sup>1a</sup> and Hamid Moosazadeh<sup>\*2</sup>

<sup>1</sup>Faculty of Mechanics, Malek Ashtar University of Technology, Tehran, Iran

<sup>2</sup>Department of Aerospace Engineering, Tarbiat Modares University, Tehran, Iran

(Received January 20, 2022, Revised August 4, 2022, Accepted August 30, 2022)

**Abstract.** The ability of baffles in increasing the sloshing damping is investigated in this study by theoretical, numerical, and experimental methods. Baffles Installed as separators in containers, can change the dynamic properties of sloshing. The main purpose of this study is to investigate the effect of baffle placement. The main purpose of this study is to investigate the effect of placing baffles in order to provide appropriate frequencies and damping and to present a practical baffle arrangement in the design of sloshing. In this regard, an experimental setup is designed to study the fluid sloshing behavior and damping properties in cylindrical tanks filled up to an arbitrary depth. A new combination of annular and sectorial baffles is employed to evaluate fluid sloshing in the tank. The results show that the proposed baffle arrangement has a desired effect on the damping and fluid sloshing frequencies and optimally satisfies the anticipated design requirements. In addition, the theoretical frequencies exceed empirical frequencies at the points far from baffles, while at the points close to baffles, the empirical ones are higher than theoretical ones. Also, at the depths near the bottom of container sloshing frequencies are not affected by sectorial baffles, although the theoretical curve predicts a reduction in the fundamental frequency of sloshing. Finally, the results of finite volume and finite element methods which compared with experimental data, indicated a good agreement between different approaches.

**Keywords:** anti-slosh baffles; circular cylindrical containers; damping ratio; finite volume method; free surface elevation; surface wave theory

## 1. Introduction

The movement of fluid in open-surface tanks is known as sloshing. This phenomenon is of great importance in many vehicles, trains carrying liquefied chemicals, liquefied petroleum vessels and spacecrafts, and may produce devastating effects if not carefully suppressed (Ibrahim 2005). Performance and stability are the most important factors in the design of fluid sloshing storage tanks. In particular, when the external excitation frequency approaches the original natural frequency, the large forces and torques generated by the fluid may result in system instability and structural failure. In practice, a variety of passive devices are used to overcome the adverse effects

---

\*Corresponding author, Ph.D., E-mail: hamid.moosazadeh@modares.ac.ir

<sup>a</sup>Assistant Professor, E-mail: Mohammadi.mm@mut.ac.ir

of sloshing and fluid movement inside a tank. A common technique is to insert additional sub-structures, called baffles or separators, into the tank in such a way as to control fluid sloshing (Budiansky 1960). Studies on the sloshing behavior of baffled tanks date back to about fifty years ago, when significant volumes of laboratory and theoretical equations focused on the effect of baffles on the sloshing of space equipment fluid. Since then, many authors have addressed this issue in containers (Budiansky 1960, Ibrahim *et al.* 2001, Ibrahim 2005, Faltinsen and Timokha 2010, Hasheminejad and Aghabeigi 2009, Hasheminejad and Mohammadi 2011, Shojaeefard *et al.* 2014, Cherif and Ouissi 2016, Cui *et al.* 2008). A brief overview of the most important works directly related to the present study is presented in what follows. Strandberg (1978) carried out an experimental study on the stability and dynamic performance of horizontal tankers with different shapes and compositions of various baffle types, and concluded that vertical baffles are preferred over unbaffled containers or containers with horizontal baffles. Evans and McIver (1987) utilized the method of expanding eigenfunctions to investigate the effect of adding a vertical baffle from the floor or from the surface into a rectangular tank. Amabili (2000) presented semi-analytical methods to investigate vibrations of plates, shells and plate-shell systems coupled with sloshing. The Rayleigh quotient of the system is used to attain expressions of symmetric formulations of the eigenvalue problem. The method is applied to a vertical, simply supported, circular cylindrical shell partially filled by an incompressible fluid. Numerical outcomes showed that there is a strong interaction between the first sloshing and bulging modes, for a fixed number  $n$  of circumferential modes, when the corresponding natural frequencies become very adjacent. Amabili (2001) introduced a new formulation for the oscillations of circular plates in contact with a free liquid surface. The fully coupled problem between sloshing modes and bulging modes of the plate is solved by means of the Rayleigh Ritz technique. He present that in case of flexible plate, a very strong interaction between the sloshing and bulging modes arises. Furthermore, the amplitude of the free-surface oscillations for the bulging modes can even be larger than the plate deflection.

Chow *et al.* (2002) adopted the structural-acoustic simultaneous finite element method (FEM) for the parametrical investigation of the eigenvalues of a circular cylindrical baffled tank. Modaresi *et al.* (2007) used Fluent to create a three-dimensional (3-D) model in baffled, non-baffled partially-filled tanks to investigate the importance of baffles on the amount of unsteady forces and moments generated by transient sloshing. Firouzabadi *et al.* (2008) performed a 3-D boundary element analysis to investigate the natural frequencies and fluid sloshing modes in finite tanks with arbitrary geometry. Eswaran *et al.* (2009) applied fluid volume techniques using Adina (an engineering simulation tool) to examine the ability of the baffles to limit sloshing power in cubic tanks. Maleki and Ziafar (2008) proposed a hydrodynamic model based on the Laplace differential equation to estimate the fluid sloshing damping ratio created by a horizontal annular baffle as well as a vertical baffle in cylindrical tanks under transverse excitation. Goodarzi and Yazdi (2010) investigated the effect of horizontal and vertical baffles on the sloshing amplitude damping in rectangular tanks. By comparing the analytical and experimental results, they showed that their derived equations are sufficiently accurate to predict sloshing damping. Akyildiz *et al.* (2013) inspected the sloshing in circular cylindrical vessels with annular baffle under rotational excitation. They demonstrated that annular baffles had a significant effect on reducing free surface oscillations. Carra *et al.* (2013) experimentally studied the dynamic response of a thin rectangular plate in contact with free surface of water- filled tanks on one or both sides, at different fluid levels, in both linear and nonlinear formulation. They showed that the plate deformation as a result of hydrostatic pressure has a noteworthy effect in varying the plate nonlinearity. Also, for excitation in the frequency closed to the natural mode of the plate, the liquid free surface

oscillation is 1/2-subharmonic amplitude. Hasheminejad *et al.* (2014) investigated the effect of horizontal and vertical baffles on the sloshing in horizontal cylindrical tanks. They showed that anti-slosh baffles play a significant role in reducing the overturning moment on the tank wall. Xue *et al.* (2017) investigated fluid sloshing in a rectangular tank with four vertical baffle types over a wide excitation frequency range. They evaluated sloshing pressure changes on the tank wall and baffles under different excitation frequencies for non-baffled tanks and tank with a bottom-mounted vertical baffle, surface-piercing vertical baffle and two types of perforated vertical baffle. Their results showed that in the frequency range of 0.4-1.4 Hz, the surface-piercing vertical baffle is a more effective tool in reducing impact pressure than bottom-mounted vertical baffle, especially near the natural frequency. Their experimental results also proved that the effect of vertical baffle on the reduction of destructive pressure depends not only on the relationship between the excitation frequency and the natural frequency, but also on its configuration and position. Arora *et al.* (2017) attributed the major cause of sloshing originated from the movement of fuel's free surface in filled containers to the design of heavy truck fuel tanks. They showed that in tanks with a capacity of up to 900 liters, this phenomenon could cause the fuel to hit the container with high forces, which puts vulnerable sections of the tank to heavy dynamic loads. In this regard, they proposed a fluid-structure interaction method by combining the finite volume and finite element model to analyze this problem. Wang *et al.* (2019) developed an analytical method for obtaining the fluid dynamic response in a circular cylindrical tank with several circular rigid baffles under torsional excitation. They introduced new generalized coordinates to represent the free-surface height of the fluid and the velocity potential function which includes the Stokes-Jukovski potential. In addition, by dividing the fluid area, a method was presented to obtain an analytical solution of their Stokes-Jokowski potential. Their parametric investigations showed that the height of surface waves increased with increasing internal radius of baffles and decreased as the top baffles went upwards. Also, the effect of fluid sloshing between baffles became apparent when the inner baffle radius was 0.7 time the external baffle radius or more. They also showed when the external excitation frequency is relatively large, the resulting force and torque chiefly depend on the angular acceleration and Stokes-Jokowski potential. Dinçer and Demir (2020) used an entirely coupled FSI method to study the hydro-elastic response of a completely submerged vertical baffled rectangular tank under far and near field seismic excitations. The elastic baffle could damp the sloshing oscillation after the excitation was over. Also, the maximum tip displacement of the elastic baffle under near fault excitations is greater than real-life El Centro earthquake. Sun *et al.* (2020) proposed a mass-spring analytical model to study of the liquid sloshing in a seismic excited baffled cylindrical tank based on soil foundation. Combined with the substructure method, the governing equation of the coupled soil-tank model is extracted. The effects of the soil property, the fluid depth and the baffle arrangement on dynamic responses and seismic behavior of the coupled structure are investigated. The results their study represent that the soil properties and the baffle configuration can have a notable effect on liquid sloshing. Recently, Baghban *et al.* (2022) used annular and horizontal baffles to investigate the baffles' relative effectiveness on the seismic response of elevated storage tanks. The structural interaction between the fluid, the horizontal and annular baffles, and the elevated sloshing container under different external excitations are studied using Abaqus software. The results of this study approve that using the baffles, the maximum shear force in flexible and rigid storage tank decreases as much as 26.43% and 31.90%, respectively, and the maximum hydrodynamic pressure reduced to 50.1% of unbaffled tank.

The above review clearly shows that although a large number of sloshing studies have been

performed on various baffled tanks, an accurate report of the simultaneous effect of annular and sectorial baffles in cylindrical fluid-filled container is lacking in the literature. In this study, a new combination of circular and sectorial baffles is designed in the fluid tanker which is used in the experimental model to optimally mitigate the fluid surface sloshing as the fluid level inside the tank decreases. The main purpose of this paper is to investigate the effect of baffle configuration on the sloshing frequencies and damping in order to propose a practical arrangement to meet the design requirements of fluid storage tanks. The obtained empirical results can also be used as fundamental data in numerical modeling. The most important innovations of this article can be summarized as follows:

- Experimental evaluation of sloshing oscillations in a tank with complex baffles and comparison of the results of different theories with experimental results.
- Providing a combination of annular and sectorial baffles to significantly increase the sloshing damping and tank stability.
- Development of a numerical model to predict sloshing frequencies and damping and comparing them to experimental results.

To this end, an experimental setup is designed to study the sloshing frequencies and damping properties of cylindrical tanks filled up to an arbitrary depth. The container is then subjected to variable frequency harmonic transverse excitation and the fluid oscillations are recorded with a camera. By analyzing the experimental results, the frequencies and damping of sloshing at different fluid depths are calculated and the effect of baffles on the sloshing properties is investigated. In addition, analytical and numerical models are developed to predict sloshing frequencies and damping, followed by a comparison with test results.

## 2. Fundamental equations

Assuming irrotational, incompressible, inviscid flow, the velocity function  $\varphi$  satisfies the Laplace equation as in (Ibrahim 2005)

$$\nabla^2 \varphi = 0. \quad (1)$$

Consider a cylindrical tank subjected to transverse harmonic excitation  $\ddot{x}(t) = \ddot{x}_0 e^{i\omega t}$ . The solution of Laplace equation under free surface boundary conditions and rigid walls is given as (Maleki and Ziyaeifar 2008)

$$\varphi = \left( \frac{g\eta}{i\omega} \right) \frac{\cosh(\lambda_1 z/R)}{\cosh(\lambda_1 H/R)}, \quad (2)$$

where  $\omega_j = \frac{\lambda_j g}{R} \tanh\left(\lambda_j \frac{H}{R}\right)$  is the natural sloshing frequency and  $\eta(r, \theta, t)$  is the free surface height (level) obtained from (Maleki and Ziyaeifar 2008)

$$\eta(r, \theta, t) = R \left[ \sum_{j=1}^{\infty} \frac{1}{1 - (\omega/\omega_j)^2} \frac{2}{\lambda_j^2 - 1} \frac{J_1(\lambda_j r/R)}{J_1(\lambda_j)} \right] \frac{\ddot{x}_0}{g} e^{i\omega t} \cos \theta, \quad (3)$$

where  $R$  is the container radius,  $H$  is the fluid height,  $g$  is the gravitational acceleration,  $J_1$  is the Bessel function of first kind, and  $\lambda_j$  are the roots of the function  $J_1'$ . The sloshing energy is obtained from classical theories in the form (Maleki and Ziyaeifar 2008)

$$E = \frac{1}{4} \rho g \eta^2 \left( 1 - \frac{1}{\lambda_1^2} \right) \pi R^2, \tag{4}$$

where  $\rho$  is the fluid density. The damping resulting from fluid sloshing is proportional to the damped energy in each cycle, and is described as (Maleki and Ziyaeifar 2008)

$$\gamma = \frac{1}{2\omega} \frac{d\bar{E}/dt}{E}, \tag{5}$$

where  $D = d\bar{E}/dt$  is the average energy depreciated in each cycle of oscillation,  $\omega$  is the sloshing frequency and  $\gamma$  is the damping ratio. For example, according to Maleki and Zeyaeifar (2008), the damping ratio is expressed as

$$\gamma_r = 4C_r \sqrt{\frac{\eta_{max}}{R}} \left( \frac{\sinh(1.84h/R)}{\sinh(1.84H/R)} \right) \tanh(1.84H/R), \tag{6}$$

where  $\gamma_r$  is the sloshing damping ratio with annular horizontal baffles,  $\eta_{max}$  is the maximum free surface height,  $h$  is the baffle height,  $r_b$  is the baffle radius and  $C_r$  is a function proportional to the baffle width which is found from (Maleki and Ziyaeifar 2008)

$$C_r = \left( \frac{r_b}{R} \right)^{1.5} \left( 2 - \frac{r_b}{R} \right). \tag{7}$$

In sloshing tanks whose free surface height is greater than tank radius, one can write (Maleki and Ziyaeifar 2008)

$$\gamma_r = 2.83e^{-4.6[d/R]} C_1^{1.5} \sqrt{\frac{\eta_{max}}{R}}, \tag{8}$$

where  $d = H - h$  is the baffle distance from the free surface and  $C_1$  is the effective baffle surface. If the baffle is completely floated in the fluid, i.e.,  $\eta/R \leq d/R$ , then  $C_1$  can be obtained from (Maleki and Ziyaeifar 2008)

$$C_1 = \frac{r_b}{R} (2 - r_b/R). \tag{9}$$

If the baffle is partially out of fluid even for a limited time, i.e.,  $\eta/R(1 - r_b/R) < d/R \leq \eta/R$ , the coefficient  $C_1$  is calculated from (Miles 1958, Bauer 1960)

$$\begin{aligned} C_1 = & \frac{r_b}{R} (2 - r_b/R) - \frac{1}{2} (1 - (d/R + (n - 1)D/R)/(\eta/R)) \\ & + \frac{2}{\pi} ((d/R + (n - 1)D/R)/(\eta/R)) \ln \left[ \frac{\eta/R + \sqrt{(\eta/R)^2 - (d/R + (n - 1)D/R)^2}}{d/R + (n - 1)D/R} \right] \\ & - \frac{1}{\pi} \frac{d/R + (n - 1)D/R}{(\eta/R)^2} \sqrt{(\eta/R)^2 - (d/R + (n - 1)D/R)^2} \\ & + \frac{1}{\pi} \sin^{-1}((d/R + (n - 1)D/R)/(\eta/R)) - \frac{1}{2} (d/R + (n - 1)D/R)/(\eta/R). \end{aligned} \tag{10}$$

Also, if the baffle is completely out of fluid and in contact with it only for some moments, i.e.,  $d/R < \eta/R(1 - r_b/R)$ , then  $C_1$  is modified as (Miles 1958, Bauer 1960)

$$\begin{aligned}
 C_1 = & r_b/R(2 - r_b/R) - \frac{1}{2}(1 - (d/R)/(\eta/R)) + \frac{2}{\pi} (d/R)/(\eta/R) \ln \left[ \frac{\eta/R + (\eta/R)^2 - (d/R)^2}{d/R} \right] \\
 & - \frac{1}{\pi} \frac{d/R}{(\eta/R)^2} \sqrt{(\eta/R)^2 - (d/R)^2} + \frac{1}{\pi} \sin^{-1}(d/R) - \frac{1}{2} \frac{d/R}{\eta/R} \\
 & + \frac{1}{2}(1 - r_b/R)^2(1 - (d/R)/((1 - r_b/R)\eta/R)) \\
 & - \frac{2}{\pi} \frac{d/R(1 - r_b/R)}{\eta/R} \ln \left[ \frac{\eta/R + \sqrt{(\eta/R)^2 - ((d/R)/(1 - r_b/R))^2}}{(d/R)/(1 - r_b/R)} \right] \\
 & + \frac{1}{\pi} \frac{d/R(1 - r_b/R)}{(\eta/a)^2} \sqrt{(\eta/R)^2 - ((d/R)/(1 - r_b/R))^2} \\
 & - \frac{1}{\pi} (1 - r_b/R)^2 \sin^{-1}((d/R)/(1 - r_b/R)\eta) + \frac{1}{2} (1 - r_b/R)(d/R)/(\eta/R)
 \end{aligned} \tag{11}$$

For a set of baffles, the sloshing damping coefficient is calculated using the superposition principle in the form

$$\gamma_r = 2.83 \sqrt{\eta_{max}/R} \left( \sum_{n=1}^N e^{-4.6(d/R + (n-1)D/R)} C_n^{1.5} + \sum_{m=1}^M e^{-4.6(\frac{mD}{R} - \frac{d}{R})} C_m^{1.5} \right), \tag{12}$$

where  $N$  is the number of submerged baffles in the fluid and  $M$  is the number of baffles outside the fluid. Also,  $C_n$  is the effective surface coefficient for the  $n$ -th baffle and if  $\eta/R \leq d/R + (n - 1)D/R$ , one can write

$$C_n = \frac{r_b}{R} (2 - r_b/R). \tag{13}$$

where  $D$  is the distance between baffles. If  $\eta/R(1 - r_b/R) < d/R + (n - 1)D/R \leq \eta/R$ , the coefficient  $C_n$  is calculated from (Bauer 1960)

$$\begin{aligned}
 C_n = & \frac{r_b}{R} (2 - r_b/R) - \frac{1}{2}(1 - (d/R + (n - 1)D/R)/(\eta/R)) \\
 & + \frac{2}{\pi} ((d/R + (n - 1)D/R)/(\eta/R)) \ln \left[ \frac{\eta/R + \sqrt{(\eta/R)^2 - (d/R + (n - 1)D/R)^2}}{d/R + (n - 1)D/R} \right] \\
 & - \frac{1}{\pi} \frac{(d/R + (n - 1)D/R)}{(\eta/R)^2} \sqrt{(\eta/R)^2 - (d/R + (n - 1)D/R)^2} \\
 & + \frac{1}{\pi} \sin^{-1}((d/R + (n - 1)D/R)/(\eta/R)) - \frac{1}{2} ((d/R + (n - 1)D/R)/(\eta/R)).
 \end{aligned} \tag{14}$$

Moreover, if  $d/R + (n - 1)D/R \leq \eta/R \left(1 - \frac{r_b}{R}\right)$ , the coefficient  $C_n$  is expressed as (Miles 1958, Bauer 1960)

$$\begin{aligned}
 C_n = & (2r_b/R - (r_b/R)^2) - \frac{1}{2}(1 - (d/R + (n-1)D/R)/(\eta/R)) + \frac{2}{\pi}((d/R + (n-1)D/R)/(\eta/R)) \ln \left[ \frac{\eta/R + \sqrt{(\eta/R)^2 - (d/R + (n-1)D/R)^2}}{d/R + (n-1)D/R} \right] - \\
 & \frac{1}{\pi} \frac{(d/R + (n-1)D/R)}{(\eta/R)^2} \sqrt{(\eta/R)^2 - (d/R + (n-1)D/R)^2} + \frac{1}{\pi} \sin^{-1}((d/R + (n-1)D/R)/(\eta/R)) - \\
 & \frac{1}{2}((d/R + (n-1)D/R)/(\eta/R)) + \frac{1}{2}(1 - r_b/R)^2 [1 - ((d/R + (n-1)D/R)/((1 - r_b/R) \eta/R))] - \frac{2}{\pi} [(d/R + (n-1)D/R)(1 - r_b/R)/(\eta/R)] \\
 & \ln \left[ \frac{\eta/R + \sqrt{(\eta/R)^2 - ((d/R + (n-1)D/R)/(1 - r_b/R))^2}}{((d/R + (n-1)D/R)/(1 - r_b/R))} \right] + \frac{1}{\pi} (d/R + [(n-1)D/R]) [(1 - r_b/R)/(\eta/R)^2] \\
 & \sqrt{(\eta/R)^2 - (d/R + (n-1)D/R)^2} / (1 - r_b/R)^2 - \frac{1}{\pi} (1 - r_b/R)^2 \sin^{-1}((d/R + (n-1)D/R)/((1 - r_b/R) \eta/R)) + \frac{1}{2} (1 - r_b/R) ((d/R + (n-1)D/R)/(\eta/R)).
 \end{aligned} \tag{15}$$

In addition, if the baffle is completely out of fluid and not in contact with it during simulation, then  $C_m = 0$ . Also, if  $\eta/R \leq mD/R - d/R$ , then  $C_m$  is expressed as (Bauer 1960)

$$\begin{aligned}
 C_m = & \frac{1}{2}(1 - (d/R + mD/R)/(\eta/R)) - \frac{2}{\pi}((mD/R - d/R)/(\eta/R)) \ln \left[ \frac{\eta/R + \sqrt{(\eta/R)^2 - (mD/R - d/R)^2}}{mD/R - d/R} \right] - \frac{1}{\pi} \frac{mD/R - d/R}{(\eta/R)^2} \sqrt{(\eta/R)^2 - (mD/R - d/R)^2} - \\
 & \frac{1}{\pi} \sin^{-1} \left( \frac{mD/R - d/R}{\eta/R} \right) + \frac{1}{2} \frac{(mD/R - d/R)}{\eta/R}.
 \end{aligned} \tag{16}$$

Finally, if  $mD/R - d/R \leq \eta/R$ , the coefficient  $C_m$  is expressed as (Miles 1958, Bauer 1960)

$$\begin{aligned}
 C_m = & (1/2)(1 - (d/R + mD/R)/(\eta/R)) - ((1/\pi)(mD/R - d/R)/(\eta/R)^2) \sqrt{(\eta/R)^2 - (mD/R - d/R)^2} - (1/\pi) \sin^{-1}(((mD/R - d/R)/(\eta/R)) + (1/2)((mD/R - d/R)/(\eta/R)) - (1/2)(1 - r_b/R)^2 [1 - ((mD/R - d/R)/((1 - r_b/R) \eta/R))] + (2/\pi)((mD/R - d/R)(1 - r_b/R)/(\eta/R)) \ln \left[ \frac{\eta/R + \sqrt{(\eta/R)^2 - ((mD/R - d/R)/(1 - r_b/R))^2}}{((mD/R - d/R)/(1 - r_b/R))} \right] - (1/\pi)(mD/R - d/R)(1 - r_b/R)/(\eta/R)^2 \sqrt{(\eta/R)^2 - (mD/R - d/R)^2} / (1 - r_b/R)^2 + (1/\pi)(1 - r_b/R)^2 \sin^{-1}((mD/R - d/R)/((1 - r_b/R) \eta/R)) - (1/2)(1 - r_b/R)((mD/R - d/R)/(\eta/R)).
 \end{aligned} \tag{17}$$

In this study, a comprehensive MATLAB code is developed to find the sloshing frequencies and damping in a cylindrical baffled tank. The code considers the circular baffle effect arranged along the tank which calculates the effect of all baffles by combining the damping and sloshing frequency equations at each moment of fluid surface variations. In addition, theoretical results are compared with both experimental and numerical results.

### 3. Experimental method

As a fluid filled tank oscillates, different sloshing waves will be generated depending on the fluid height and frequency. The intensity of sloshing and its additional dynamic pressure depend on the tank geometry, the fluid height, the amplitude and nature of the tank excitation. They also depend on the frequency of excitation especially at frequencies close to the fundamental frequency of the tank. To achieve a better understanding of different aspects of sloshing and estimate the variations of wave height, an experimental setup is planned for the cylindrical tank. The focus of this section is on the experimental study of sloshing damping and determination of the first and second natural frequencies. According to the required damping profiles (with a maximum of 0.05),

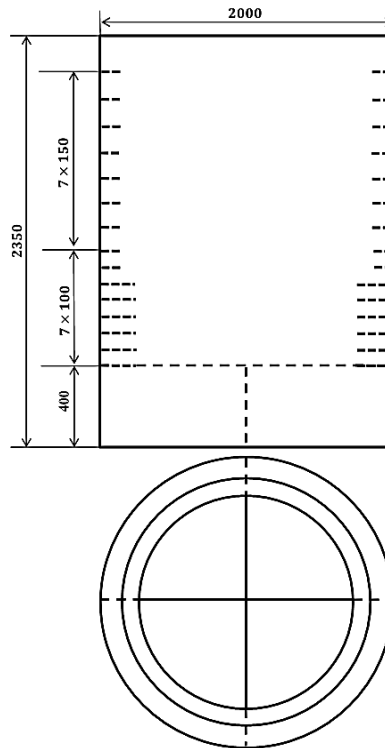


Fig. 1 A baffled cylindrical fuel tank

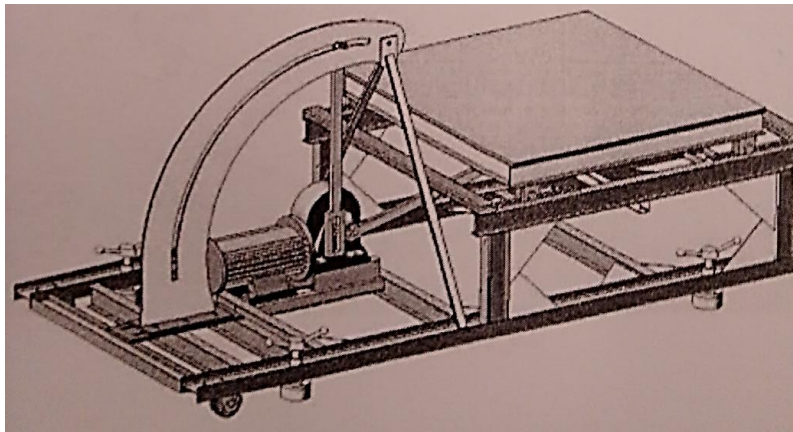


Fig. 2 Movable table

the design of damper baffles in view of the increase in the sloshing damping is performed based on the available scientific literature and previous experiments. The proposed methodology benefits from annular baffles which exhibit a superior performance. In addition, the tank ends are sectioned using perpendicular sectorial baffles. This approach increases both the damping and the frequency of sloshing. A fuel tank (filled with colored water) along with the designed baffles is displayed in Fig. 1.



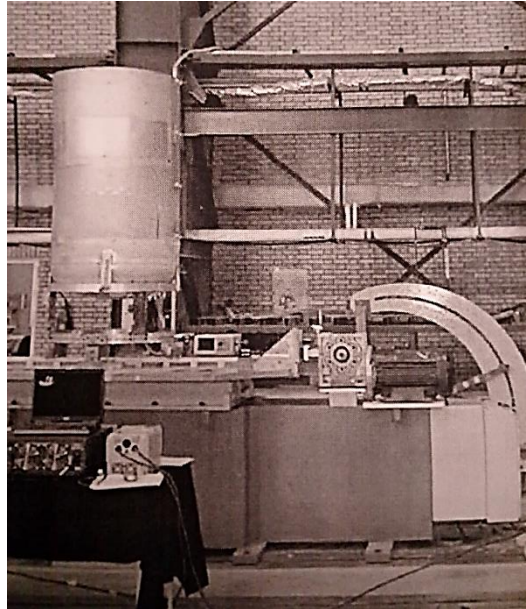


Fig. 3 Sloshing tank under excitation

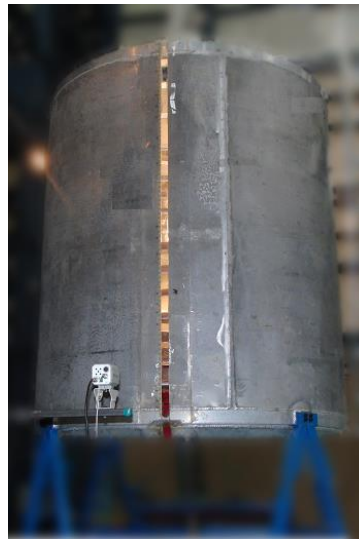


Fig. 4 Amplitude recording with camera

As observed in Fig. 1 (all dimensions in millimeters), there are nine circular annular baffles with the width of 5 cm and nine circular annular baffles with the width of 3 cm along the tank. The tank bottom is divided into four parts (four sectorial baffles) with two 3-mm thickness plates of the height of almost 400 mm. After the construction of reservoirs and preparation of test equipment, the tank is mounted on a movable table with dimensions of 2.5 meters wide and 3 meters long, which is able to shake the tank with a desired amplitude and frequency.

The excitation table is shown in Fig. 2. The table is connected to a four-bar mechanism that

converts the variable-frequency rotary motion of the motor into transverse excitation into the tank. The tank mounted on the table is shown in Fig. 3.

The container then undergoes variable frequency harmonic transverse excitation. The displacement of movable table is adjusted such that the fluid level is visible but remains in the linear range. During frequency sweep excitation, the frequency at which the maximum sloshing amplitude (based on the recorded image) is observed is considered as the natural frequency. The test requirements include the first and second natural frequencies as well as the sloshing damping at predefined levels of liquid fill height. In fact, the tank is filled up to predetermined levels and the frequencies and damping for each height are then calculated. The sloshing amplitude is recorded by precision cameras from a transparent graduated groove (made of acrylic glass) created on the tank (Fig. 4).

The tank is placed on a lateral horizontal excitation table (Fig. 3) which provides constant amplitude and different frequencies over the range 0.3-2.5 Hz with steps of 0.1 Hz. If one seeks a better recording by the installed cameras, the excitation amplitude at the desired frequency should provide a sloshing amplitude in the range  $4 \leq \eta \leq 6$  cm. Nonetheless, the amplitude must remain in the linear range. Also, the amplitude of fluid sloshing should be recorded by means of dynamic pressure gauges, while the lateral force caused by the fluid is registered by means of load cells installed around the tank support (Fig. 5). When the amplitude of the sloshing force and the amplitude of sloshing free surface reach their maximum values, the test is repeated with frequency intervals of 0.02 Hz.

In addition, to measure the damping associated with sloshing, a horizontal lateral excitation with a frequency close to the first natural frequency ( $0.95f_1 \leq f \leq 1.05f_2$  Hz), estimated from the previous step, is applied to the tank. Higher modes are damped quickly and do not generate a critical damping state. In this part of the test, the excitation amplitude must yield a sloshing oscillation amplitude in the range  $5 \leq \eta \leq 7$  cm. After the fluid sloshing reaches a steady state, the excitation is stopped. The stop time at each frequency is about 60 seconds. Due to its stored energy, the fluid freely continues its oscillation and the amplitude diminishes owing to the

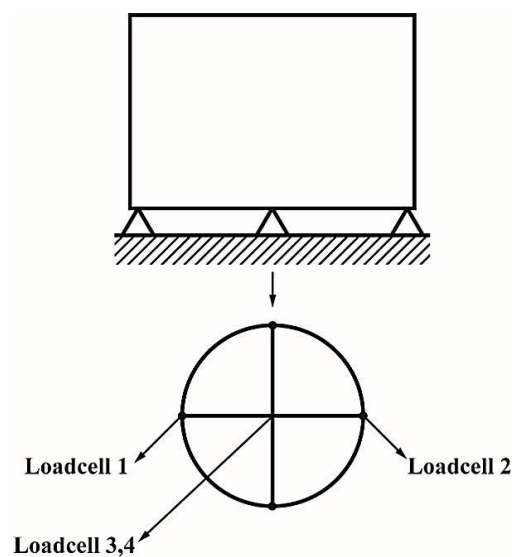


Fig. 5 Installation of load cells

damping. Over this period, the lateral force acting on the container as well as the amplitude of fluid sloshing is recorded at specific points on the tank wall in the time domain. The relation describing the logarithmic amplitude of damping is then calculated. Data recording should be continued until the sloshing is eliminated. To attain acceptable reliability, the process is repeated three times. In general, the modified logarithmic decrement equation (Bauer 1960) is applied for calculating the damping as in

$$\gamma = \frac{1}{2\pi k} \text{Ln} \frac{\eta_j}{\eta_{j+k}}, \quad (18)$$

in which  $\eta_j$  and  $\eta_{j+k}$  are the sloshing amplitudes in the  $j$ th and  $(j+k)$ th cycles of oscillation. Accordingly, the image of surface oscillation and modified logarithmic decrement equation are employed. However, the effect of higher mode shapes on the fluctuation of surface sloshing is significant and should be considered carefully. It is important to note that the use of filters (either low-pass or high-pass) to remove noise or higher frequencies alters the nature of signal damping, and the use of filter is thus not allowed. It should be noted that the presented estimation of analytical damping for damper baffles are expressed in terms of sloshing amplitude. Therefore, if the force signal is used, the correspondence of the force and the amplitude of sloshing should be identified by comparing the force and the image.

#### 4. Numerical simulation

In this section, a numerical analysis is performed using Ansys-Fluent CFD package. The VOF multiphase model with NITA scheme using the Fractional (FSM) Method is employed. The motion of domain boundaries is simulated aided by the dynamic mesh model using a UDF module. Other modeling specifications are as follows: 3-D model, double precision, pressure-based, and 0.001-sec time step. Multi-block grid is considered as hybrid T-Grid cells in all deformable blocks. A maximum of 320000 elements are selected for simulation for optimized precision and computational cost. In addition, Ansys is used to determine the natural frequency of sloshing for two different heights. The fluid is modeled using FLUID-80 element with three degrees of freedom (DoFs) per node. All nodes on wall boundaries have zero DoF. The FLUID-80 element employs the lumped-mass matrix and the reduced method for modal analysis. The reduced method only works with the masters DoF. The experimental and numerical results are compared in the next section.

#### 5. Results and discussion

The sloshing test is conducted at an acceleration of 1 g corresponding to the earth's surface gravity. Changes in the theoretical natural frequencies with respect to liquid height from the bottom of tank are shown in Fig. 6, where the experimental frequencies for predefined levels, determined by testing and relative error (theory toward experiment), are presented.

As one can see, the theoretical curve follows the experimental data. Both frequencies have a decreasing trend, from high levels to a height of about 45 cm, which is related to the height reduction of the free surface of fluid from the bottom of tank. Experimental frequencies are lower

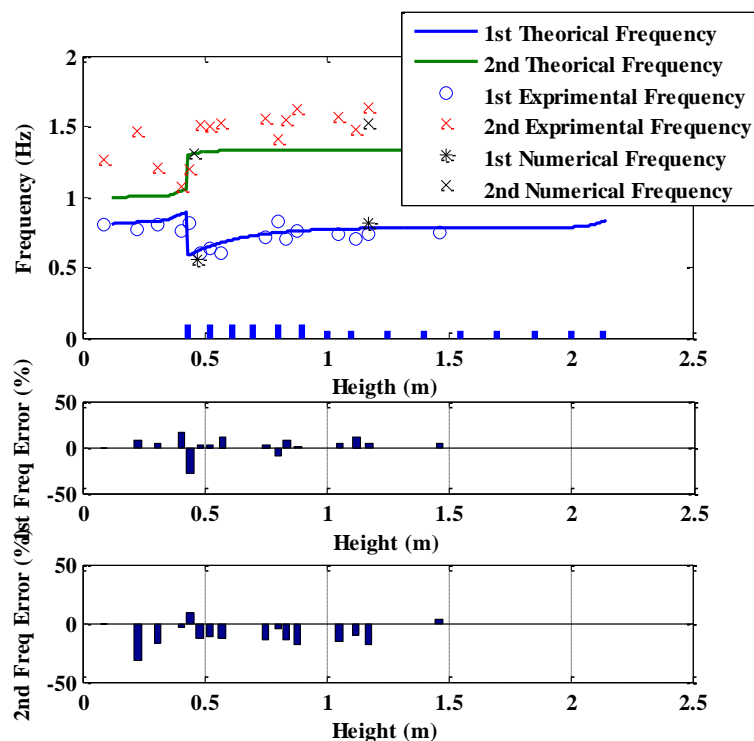


Fig. 6 Theoretical natural frequencies of the first and second sloshing modes, as well as experimental and numerical frequencies at different levels with relative error in the fuel tank

than theoretical ones for the points far from baffles (e.g., between two baffles), but greater in areas close to baffles, and they are higher than theoretical frequencies in some areas. From the approximate height of less than 45 cm, the first frequency increases and the second frequency decreases. These changes, initiated from the effect of sectorial baffles, are clearly visible in experimental data. At most test levels, the experimental and theoretical frequencies have a difference of less than 15% and 20%, respectively. A good agreement has been observed between the experimental results and the analytical theory for the first frequency of the baffled and the segmental parts. The difference between the theoretical and experimental results is in the second frequency, which has nothing to do with height, and in all situations, i.e., the baffled section and the segmental section, a clear and almost constant difference between theoretical and experimental results has been observed. For the part with a circular baffle with a height of more than 0.5 meters, the value of the second dimensionless frequency is 1.3 and the value specified experimentally shows the value of 1.5. The error rate will be around 12%. In the segmental part with a height of less than 0.5 meters, the value of the theoretical second frequency is between 1 to 1.1 and the value of the experimental frequency (except for one point with a higher value and one point in accordance with the theory) between 1.2 to 1.3. Therefore, the error rate of this part is 16%. It should also be noted that by passing from the baffled section to the segmental section, a second frequency drop is observed in the theoretical and experimental models, and both go through the same process.

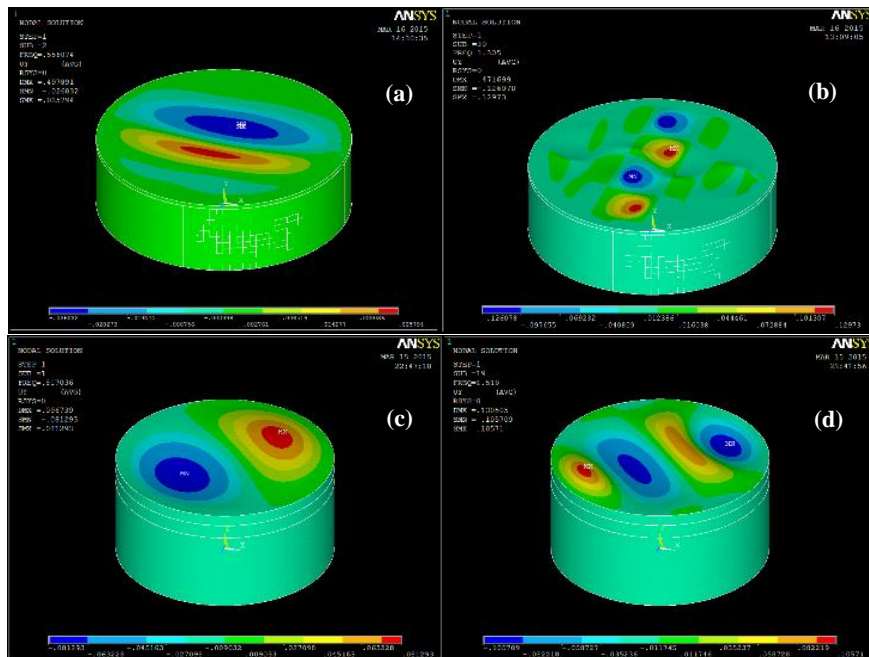


Fig. 7 First two mode shapes of sloshing in the fuel tank: (a) first mode of sloshing in the tank with liquid height=0.46 m, (b) second mode of sloshing in the tank with liquid height=0.46 m, (c) first mode of sloshing in the tank with liquid height=1.15 m, second mode of sloshing in the tank with liquid height=1.15 m

There are several reasons for this discrepancy between the second theoretical and experimental frequency:

- Changing from circular baffle to sectoral will cause an error. Because in theory, only the annular or segmental baffle model has been studied separately.
- Due to the simplicity of the first mode and the greater the effective moving mass in this mode, not much difference has been observed for the first mode. However, with the reduction of the effective mass in the second mode and the more complex deformation of the second mode, the possibility of creating differences between the results has increased. Therefore, the sensitivity of the experimental device will be higher in the second mode and the difference in the second mode will be more than the first mode.
- In the experimental results, the effects of three-dimensional nature of the fluid surface and the surface motion of the fluid are observed, which has been omitted in theory.

Moreover, as Fig. 6 shows, there is a good agreement between numerical and experimental results. Next, the theoretical damping after implementing the designed baffles in (Miles 1958, Maleki and Ziyaeifar 2008) is recalculated according to the criteria for provided damping  $\eta_m/R \cong 0.02$ . Also, the experimental damping is calculated for the fluid surface sloshing amplitude  $\eta_m \cong 0.02R$ . In addition, the results of numerical study on frequency and the corresponding mode shapes are shown in Fig. 7.

The theoretical damping with respect to fluid level (i.e., different water heights) is shown in Figure 8 for the fuel tank. In addition, the required damping and calculated damping from the experimental results for the fuel tank are given in this figure. As shown in Fig. 6, the damping

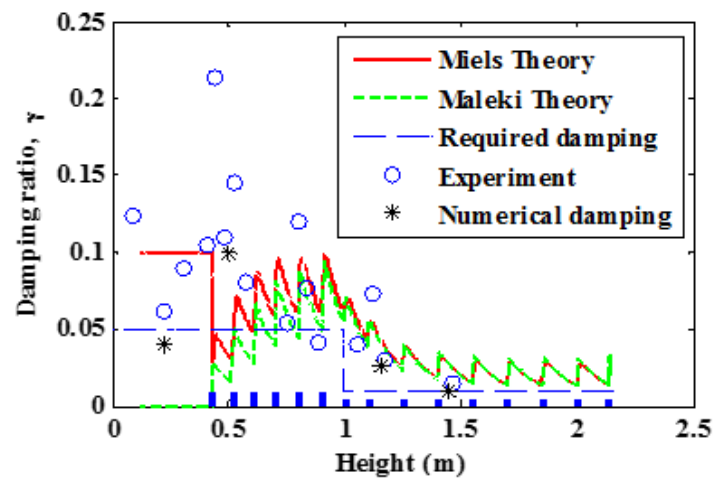


Fig. 8 Theoretical sloshing damping curve in the fuel tank and experimental damping at different levels

changes in a sawtooth way with respect to the fluid height from the bottom of tank. The experimental damping approximately follows the trend of theoretical damping. However, the experimental damping is smaller at points corresponding to the minimums of theoretical curve or between baffles. The amount of this difference is probably related to the overestimation of analytical formula or disregarding the superposition principle for the damping of sequential baffles.

In contrast, the experimental damping is larger at points corresponding to the maximums of theoretical curve. Therefore, the experimental damping shows severe local fluctuations in the fluid surface passing through the baffle.

At the depths near the bottom of tank outside of the repositories sector (e.g., height=45-90 cm), the damping generally decreases according to the theoretical curve, while the experimental frequency increases in terms of its average value. This increase stems from the effect of sectorial baffles at higher fluid levels. By comparing the experimental damping and required damping, one concludes that the baffles satisfy the required damping. In addition, the numerical simulation results of the free surface oscillations at the point of contact with the wall for the four depths 0.2, 0.5, 1.15, and 1.5 m are shown in Fig. 9(a)-(d), respectively. Then, using Eq. (18), the free surface oscillation damping is calculated. As shown in Fig. 6, damping outputs present a modest agreement with the findings of experimental approach. Finally, it can be said that numerical and experimental results have shown a fair agreement. By reducing the height and comparing the damping results between 1.5 to 0.6, an increase in damping is well observed in the theoretical and experimental models. However, with a more reduction in height between 0.6 and 0.4 due to the use of annular baffle damping theory without considering the segmental baffle, we have observed a damping reduction in the theoretical model. While in the experimental model, the presence of a segmental baffle has increased the damping in this range.

## 7. Conclusions

The potential of baffles in increasing the hydrodynamic damping of sloshing in circular

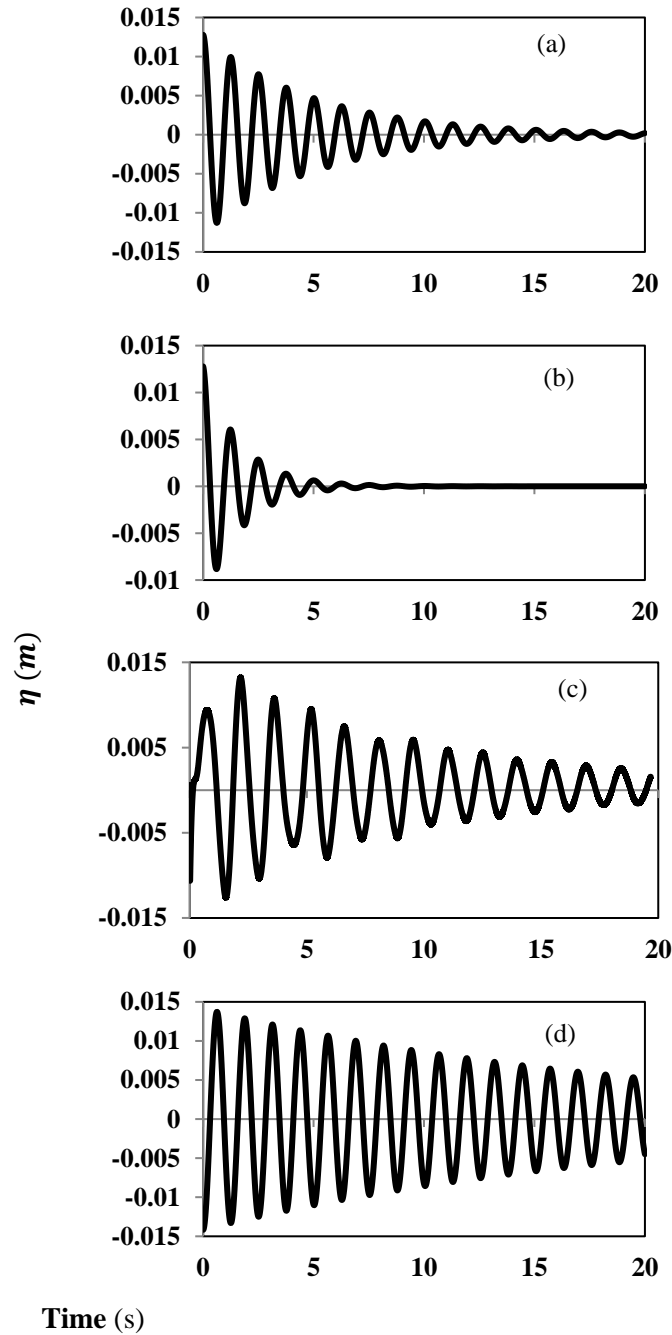


Fig. 9 Numerical time history of free surface elevation in the fuel tank for different liquid heights

cylindrical storage tank with various fill levels and specific baffle configurations was investigated experimentally and numerically. A series of experiments using a tank model on a shake table was

carried out and the results were compared with analytical equations. In addition, the numerical damping/frequency study using a commercial CFD/FEM package was performed. The results were then compared to theoretical and experimental data.

The most important findings of this study through accurate observations are summarized as follows.

- There is a fairly good agreement between theoretical and experimental frequencies. The theoretical curve follows the experimental data. Both frequencies have a decreasing trend, from high levels to a height of about 45 cm, attributed to the reduction in the free surface height of fluid measured from the bottom of tank.
- Experimental frequencies are lower than theoretical ones for the points far from baffles (e.g., between two baffles), while they are greater than their theoretical counterparts in the proximity of baffles. From the approximate height of less than 45 cm, the first frequency increases and the second frequency decreases. These changes are affected by sectorial baffles, as clearly visible in experimental data. At most test levels, the first experimental and theoretical frequencies have a difference of less than 15% and 20%, respectively.
- The damping changes in a sawtooth way with respect to fluid height from the bottom of tank. Experimental damping approximately follows the trend of theoretical damping. However, the experimental damping is smaller at points corresponding to the minimums of theoretical curve or between baffles. This difference is probably related to the overestimation of analytical equation or disregarding the superposition principle.
- Miles theory, which is closer to experimental data at lower depths, predicts higher dampings than Maleki's theory.
- In addition, the results of numerical damping exhibit reasonably good agreement with the data obtained from the experimental approach.
- In view of experimental/numerical results, annular and sectorial baffles provide a high damping levels at the ends of the tank.

## References

- Akyıldız, H., Ünal, N.E. and Aksoy, H. (2013), "An experimental investigation of the effects of the ring baffles on liquid sloshing in a rigid cylindrical tank", *Ocean Eng.*, **59**, 190-197. <https://doi.org/10.1016/j.oceaneng.2012.12.018>.
- Amabili, M. (2000), "Eigenvalue problems for vibrating structures coupled with quiescent fluids with free surface", *J. Sound Vib.*, **231**(1), 79-97. <https://doi.org/10.1006/jsvi.1999.2678>.
- Amabili, M. (2001), "Vibrations of circular plates resting on a sloshing liquid: solution of the fully coupled problem", *J. Sound Vib.*, **245**(2), 261-283. <https://doi.org/10.1006/jsvi.2000.3560>.
- Arora, S. and S. Vasudevan (2017), "Analysis of sloshing-induced loads on the fuel tank structure", Diploma Work, Department of Applied Mechanics, Chalmers University of Technology, Gteborg, Sweden.
- Baghban, M.H., Razavi Tosee, S.V., Valerievich, K.A., Najafi, L. and Faridmehr, I. (2022), "Seismic analysis of baffle-reinforced elevated storage tank using finite element method", *Build.*, **12**(5), 549.
- Bauer, H.F. (1960), *Theory of the Fluid Oscillations in a Circular Cylindrical Ring Tank Partially Filled with Liquid*, National Aeronautics and Space Administration.
- Budiansky, B. (1960), "Sloshing of liquids in circular canals and spherical tanks", *J. Aerosp. Sci.*, **27**(3), 161-173.
- Carra, S., Amabili, M. and Garziera, R. (2013), "Experimental study of large amplitude vibrations of a thin plate in contact with sloshing liquids", *J. Fluid. Struct.*, **42**, 88-111.



- <https://doi.org/10.1016/j.jfluidstructs.2013.05.013>.
- Cherif, S.M.H. and Ouissi, M.N. (2016), "Free vibration analysis of a liquid in a circular cylindrical rigid tank using the hierarchical finite element method", *Lat. Am. J. Solid. Struct.*, **13**(7), 1265-1280. <https://doi.org/10.1590/1679-78251774>.
- Cho, J.R., Lee, H.W. and Kim, K.W. (2002), "Free vibration analysis of baffled liquid-storage tanks by the structural-acoustic finite element formulation", *J. Sound Vib.*, **258**(5), 847-866. <https://doi.org/10.1006/jsvi.2002.5185>.
- Cui, Y. and Liu, H. (2008), "Numerical simulation of sloshing in two dimensional rectangular tanks with SPH", *Chin. J. Hydrodyn.*, **23**(6), 618-624.
- Dinçer, A.E. and A. Demir (2020), "Application of smoothed particle hydrodynamics to structural cable analysis", *Appl. Sci.*, **10**(24), 8983. <https://doi.org/10.3390/app10248983>.
- Eswaran, M., Saha, U.K. and Maity, D. (2009), "Effect of baffles on a partially filled cubic tank: Numerical simulation and experimental validation", *Comput. Struct.*, **87**(3-4), 198-205. <https://doi.org/10.1016/j.compstruc.2008.10.008>.
- Evans, D.V. and McIver, P. (1987), "Resonant frequencies in a container with a vertical baffle", *J. Fluid Mech.*, **175**, 295-307. <https://doi.org/10.1017/S0022112087000399>.
- Faltinsen, O.M. and Timokha, A.N. (2010), "A multimodal method for liquid sloshing in a two-dimensional circular tank", *J. Fluid Mech.*, **665**, 457-479. <https://doi.org/10.1017/S002211201000412X>.
- Firouz-Abadi, R.D., Haddadpour, H., Noorian, M.A. and Ghasemi, M. (2008), "A 3D BEM model for liquid sloshing in baffled tanks", *Int. J. Numer. Meth. Eng.*, **76**(9), 1419-1433. <https://doi.org/10.1002/nme.2363>.
- Goudarzi, M.A., Sabbagh-Yazdi, S.R. and Marx, W. (2010), "Investigation of sloshing damping in baffled rectangular tanks subjected to the dynamic excitation", *Bull. Earthq. Eng.*, **8**(4), 1055-1072. <https://doi.org/10.1007/s10518-009-9168-8>.
- Hasheminejad, S. M. and Aghabeigi, M. (2009), "Liquid sloshing in half-full horizontal elliptical tanks", *J. Sound Vib.*, **324**(1-2), 332-349. <https://doi.org/10.1016/j.jsv.2009.01.040>.
- Hasheminejad, S.M. and Mohammadi, M.M. (2011), "Effect of anti-slosh baffles on free liquid oscillations in partially filled horizontal circular tanks", *Ocean Eng.*, **38**(1), 49-62. <https://doi.org/10.1016/j.oceaneng.2010.09.010>.
- Hasheminejad, S.M., Mohammadi, M.M. and Jarrahi, M. (2014), "Liquid sloshing in partly-filled laterally-excited circular tanks equipped with baffles", *J. Fluid. Struct.*, **44**, 97-114. <https://doi.org/10.1016/j.jfluidstructs.2013.09.019>.
- Ibrahim, R.A. (2005), *Liquid Sloshing Dynamics: Theory and Applications*, Cambridge University Press.
- Ibrahim, R.A., Pilipchuk, V.N. and Ikeda, T. (2001), "Recent advances in liquid sloshing dynamics", *Appl. Mech. Rev.*, **54**(2), 133-199. <https://doi.org/10.1115/1.3097293>.
- Maleki, A. and Ziyaeifar, M. (2008), "Sloshing damping in cylindrical liquid storage tanks with baffles", *J. Sound Vib.*, **311**(1-2), 372-385. <https://doi.org/10.1016/j.jsv.2007.09.031>.
- Miles, J.W. (1958), "Ring damping of free surface oscillations in a circular tank", *J. Appl. Mech.*, **25**(2), 274-276. <https://doi.org/10.1115/1.4011756>.
- Modaressi-Tehrani, K., Rakheja, S. and Stiharu, I. (2007), "Three-dimensional analysis of transient slosh within a partly-filled tank equipped with baffles", *Vehic. Syst. Dyn.*, **45**(6), 525-548.
- Shojaeefard, M.H., Talebitooti, R., Satri, S.Y. and Amiryoony, M.H. (2014), "Investigation on natural frequency of an optimized elliptical container using real-coded genetic algorithm", *Lat. Am. J. Solid. Struct.*, **11**(1), 113-129. <https://doi.org/10.1590/S1679-78252014000100007>.
- Strandberg, L. (1978), *Lateral Stability of Road Tankers: Vol. 2 Appendices*, Statens Väg-och Trafikinstitut.
- Sun, Y., Zhou, D., Amabili, M., Wang, J. and Han, H. (2020), "Liquid sloshing in a rigid cylindrical tank equipped with a rigid annular baffle and on soil foundation", *Int. J. Struct. Stab. Dyn.*, **20**(03), 2050030. <https://doi.org/10.1142/S0219455420500303>.
- Wang, J., Wang, C. and Liu, J. (2019), "Sloshing reduction in a pitching circular cylindrical container by multiple rigid annular baffles", *Ocean Eng.*, **171**, 241-249.
- Xue, M.A., Zheng, J., Lin, P. and Yuan, X. (2017), "Experimental study on vertical baffles of different

configurations in suppressing sloshing pressure”, *Ocean Eng.*, **136**, 178-189.

EC

## Nomenclature

Symbol	Description
$C_r$	Relative baffle width
$E$	Total energy of sloshing wave
$D$	Energy dissipation rate
$g$	Acceleration due to gravity
$H$	Liquid height
$h$	Baffle height
$j, k$	Dummy indices
$R$	Tank radius
$r_b$	Baffle width
$r, \theta$	Physical coordinate domain
$t$	Time
$\ddot{x}_0$	Lateral acceleration amplitude
$z$	Abcissa in physical domain
$\gamma$	Damping ratio of sloshing
$\eta$	Free surface elevation
$\lambda$	Eigenvalue
$\rho$	Fluid density
$\varphi$	Velocity potential
$\omega$	Circular frequency of the oscillations (rad/sec)